Article

Not peer-reviewed version

RNA-Seq of Nasopharyngeal Swabs from ICU Patients Infected with SARS-CoV-2 Omicron Sublineages in Adelaide, Australia, 2022–2023

Agnes Carolin , Cameron R Bishop , Branka Grubor-Bauk , Mark P Plummer , Eamon Raith , Simon C Barry , Christopher M Hope , Wilson Nguyen , Daniel J Rawle * , Andreas Suhrbier *

Posted Date: 5 September 2025

doi: 10.20944/preprints202509.0565.v1

Keywords: SARS-CoV-2; COVID-19; omicron; BA.5; XBC; nasopharyngeal; ciliated epithelia; RNASeq; viral load; patient; intensive care unit

Article

RNA-Seq of Nasopharyngeal Swabs from ICU Patients Infected with SARS-CoV-2 Omicron Sublineages in Adelaide, Australia, 2022–2023

Agnes Carolin [1,2,†], Cameron R Bishop [1,†], Branka Grubor-Bauk [3], Mark P Plummer [3,4], Eamon Raith [3,4], Simon C Barry [3], Christopher M Hope [3], Wilson Nguyen [1], Daniel J Rawle [1,*,‡] and Andreas Suhrbier [1,5,*,‡]

[1] Infection and Inflammation Department, QIMR Berghofer, Brisbane, Queensland. 4029, Australia
[2] Faculty of Health, Medicine and Behavioural Sciences, University of Queensland, St. Lucia, QLD 4072, Australia
[3] Viral Immunology Group, Adelaide Medical School, Faculty of Health and Medical Sciences, University of Adelaide, Adelaide, South Australia 5005, Australia
[4] Intensive Care Unit, Royal Adelaide Hospital, Adelaide, South Australia, 5000, Australia
[5] GVN Center of Excellence, Australian Infectious Disease Research Centre, Brisbane, QLD 4029 and 4072, Australia
* Correspondence: Daniel.Rawle@qimrberghofer.edu.au (D.J.R.); Andreas.Suhrbier@qimrberghofer.edu.au (A.S.)
† These authors should be considered joint first.
‡ These authors should be considered joint last.

Abstract

COVID-19 diagnostic testing generally involves collection of patient samples via nasopharyngeal swabs. Herein we describe viral and human gene expression data available from such samples using RNA-Seq and bioinformatics. Swabs were collected from 38 patients admitted to an Australian intensive care unit (ICU) from October 2022 to August 2023. During this time the omicron sublineages changed from BA.5, BA.2-like, XBB-like to XBC. RNA-Seq viral read data correlating well with RT-PCR-based quantitation and sublineage identification. High viral loads were associated with patients >64 years of age. Treatment with corticosteroids or baricitinib did not significantly influence viral loads. Viral loads did not correlate with length of stay in hospital or ICU, or with vaccination status. Analyses of human gene expression data were complicated by the very large range (>5 log) and variability in viral reads. Nevertheless, comparison of XBC and BA.5 samples that had comparable viral read counts, revealed differentially expressed genes and a cellular deconvolution signature that indicated increased infection of ciliated epithelial cells by XBC. A key feature that differentiated the omicron lineage from previous lineages was the increased targeting of ciliated epithelia in the upper respiratory track. The data presented herein argue that this evolutionary trend continued in the omicron sublineages.

Keywords: SARS-CoV-2; COVID-19; omicron; BA.5; XBC; nasopharyngeal; ciliated epithelia; RNA-Seq; viral load; patient; intensive care unit

1. Introduction

SARS-CoV-2, the virus that causes COVID-19, has evolved substantially since its emergence in late 2019 [1], with the omicron lineage emerging in 2022 and markedly diversifying into a series of sublineages [2–5]. Ongoing mutations in the spike protein are central to the classification of sublineages and are associated with increased transmissibility, immune evasion and receptor binding [6,7]. Other SARS-CoV-2 genes [8] are also undergoing evolutionary changes [9] that impact a range of virus-host interactions [10–12]. Omicron lineage viruses were characterized by increased

 doi:10.20944/preprints202509.0565.v1

replication in the upper (versus the lower) respiratory track [12] and a great capacity to infect ciliated epithelial cells [13,14] when compared with earlier lineage viruses. Targeting these cells facilitates viral transit across the mucus layer, as well as disrupting mucocilary clearance [15,16].

SARS-CoV-2 infection is generally diagnosed by RT-PCR or protein-based diagnostic tests performed on material collected from patients via nasopharyngeal swabs [17,18]. Such sampling collects not only viral RNA and protein, but also host cells and cellular debris from the nasopharyngeal track. Such swabs thus provide a readily available source of both viral RNA and human cellular mRNA from a major site of infection in COVID-19 patients [19]. We thus sought to determine what information might be gleaned by RNA-Seq analysis of nasopharyngeal swabs, correlating the data with patient information, with the aim of increasing the understanding of nasopharyngeal infections by omicron sublineages in humans.

2. Materials and Methods

2.1. Ethics and Regulatory Statement

Informed consent was obtained from all patients involved in the study. Nasopharyngeal swabs were collected from 49 COVID-19 patients admitted to the ICU of the Royal Adelaide Hospital from October 2022 to August 2023. Swabs were placed into TRIzol® reagent (Invitrogen) and stored at -80°C prior to transport to QIMR Berghofer. Approval was obtained from the Central Adelaide Local Health Network (CALHN) Human Research Ethics Committee (CALHN13050). Approval was also obtained from the QIMR Berghofer Human Research Ethics Committee (Ref: P3600), with all samples and patient data deidentified prior to being sent to QIMR Berghofer. Research at QIMR Berghofer was approved by the Institutional Safety Committee.

2.2. RNA-Seq and Bioinformatics

RNA was extracted from TRIzol according to manufacturer's instructions. DNAse I treatment (New England Biolabs) and RNA clean-up was undertaken using RNeasy MinElute Cleanup Kit (QIAGEN), according to the manufacturer's instructions. The Agilent 4200 Tape Station was used to provide RIN scores. Library preparations and ribosomal RNA depletions were undertaken using TrueSeq Stranded Total RNA Sample Preparation Kit, with Ribo-Zero (Illumina). Tape Station D1000 Screen Tape was used to assess the fragment size of the completed libraries; samples where cDNA amplicons could not be detected did not progress to sequencing. ThermoFisher Qubit 4 Fluorometer was used to measure the concentration of the completed libraries. Sequencing was performed using NextSeq 2000 using the flow cell P3 Reagent (200 cycles), providing 76 bp paired-end reads. All samples were run in a single sequencing run; Q30 was 89.97%.

STAR aligner was used to align the RNA-Seq reads to a combined SARS-CoV-2 BA.5 (GenBank: OP604184.1) and human (GRCh38, version 38) reference genome [20]. Samtools v1.16 [21] was used to generate viral read counts expressed as viral reads per million reads (RPM). RSEM v1.3.1 was used to generate read counts for host genes; differentially expressed genes (DEGs) were identified using DESeq2 v1.40.2 [22]. DEGs were analyzed using Ingenuity Pathway Analysis (IPA, v84978992) (QIAGEN). Relative abundance of specific cell types was estimated via cellular deconvolution using the SpatialDecon package in R [23,24], with cell-type expression matrices obtained from the human lung cell atlas [25] (https://data.humancellatlas.org/explore/projects/c4077b3c-5c98-4d26-a614-246d12c2e5d7).

2.3. RT-qPCR of Nasopharyngeal Samples

cDNA synthesis (from the purified RNA from the nasopharyngeal swab samples) was undertaken using ProtoScript II First Strand cDNA Synthesis Kit (New England Biolabs). RT-qPCR was performed using iTaq Universal Probes Supermix (Bio-Rad) and SARS-CoV-2 (Sarbeco-E) primers; Forward: 5′-ACAGGTACGTTAATAGTTAATAGCGT-3′, Reverse: 5′-

 doi:10.20944/preprints202509.0565.v1

ATATTGCAGCAGTACG CACACA -3′ [26]. The florescent probe was 5′-FAM-ACACTAGCCATCCTTACTGCGCTTCG- ZEN™/Iowa Black® FQ-3′ (Integrated DNA Technologies Australia). BioRad CFX96 was used to perform RT-qPCR with the following cycling conditions: incubation at 50°C for 10 min, followed by 3 min at 95°C, then 40 cycles of 15 secs at 95°C and 30 secs at 60°C.

2.4. Phylogenetic Tree Generation

The Integrative Genomics Viewer (IGV; v.2.9.4) [27] was used to align the viral sequences retrieved from RNA-Seq to the original SARS-CoV-2 strain. Consensus spike sequences were extracted from IGV, followed by translation via Expasy (online tool: https://web.expasy.org/translate/). MegaX (v.11) was used to generate the phylogenetic tree. Sublineages were classified further based on their spike mutations using GISAID.

2.5. Statistics

Correlations were undertaken using SPSS Statistics (v23) (IBM). Fischer's exact tests were performed using JNP Pro (SAS Institute, Cary, North Carolina, USA).

3. Results

3.1. Omicron Sublineages and Viral Read Counts from COVID-19 ICU Patients

Human nasopharyngeal swab samples were obtained from consented COVID-19 patients admitted to the Intensive Care Unit (ICU) at the Royal Adelaide Hospital between October 2022 and August 2023. The virus sublineages from patients were classified by the diagnostic laboratory at the hospital using RT-PCR of nasopharyngeal swab samples, with viral infections grouped into four omicron sublineages (Fig. 1a, x axis).

Nasopharyngeal swab samples from 49 patients were collected into TRIzol® reagent and were transported to QIMR Berghofer. RNA was isolated, with 38 patient samples yielding sufficient RNA ($\geq$100 ng) for library preparation and RNA-Seq (Table S1). Viral read counts, expressed as viral reads per million (RPM), for this patient cohort ranged across >5 logs, with levels >5000 viral RPM only seen in patients infected with BA.5 and BA.2-like sublineage viruses (Fig. 1a, yellow box). These higher viral loads were associated with age $\geq$ 64 years (see below).

RNA-Seq of 19/38 patient samples yielded sufficient spike sequence data to confirm the prior RT-PCR-based sublineage identification (Fig. 1a, black circle outlines). The variant or sublineage for four samples could not be established by either RNA-Seq (insufficient reads) or by the hospital diagnostic laboratory (Fig. 1a, Unknown).

3.2. Quantitation by RT-qPCR Correlated Well with Viral read Counts

The same purified RNA samples that were used for RNA-Seq were also analyzed by quantitative reverse transcription polymerase chain reaction (RT-qPCR) using the standard SARS-CoV-2 Sarbeco-E primers [26]. Viral RPM obtained from RNA-Seq correlated well with Cq values from RT-qPCR; viral RNA quantitation by these two methods thus provided highly comparable results.

3.3. Phylogenetic Tree of Omicron Sublineages

Of the 38 samples analyzed by RNA-Seq, 19 provided sufficient spike sequence data to allow construction of a phylogenetic tree (Fig. 1c). Clear clustering of the sublineages was evident, reflecting the groupings applied in Fig. 1a. As might be expected, XBF, a recombinant of BA.5.2 and BA.2.75 [28], grouped with the BA.2-like viruses.

 doi:10.20944/preprints202509.0565.v1

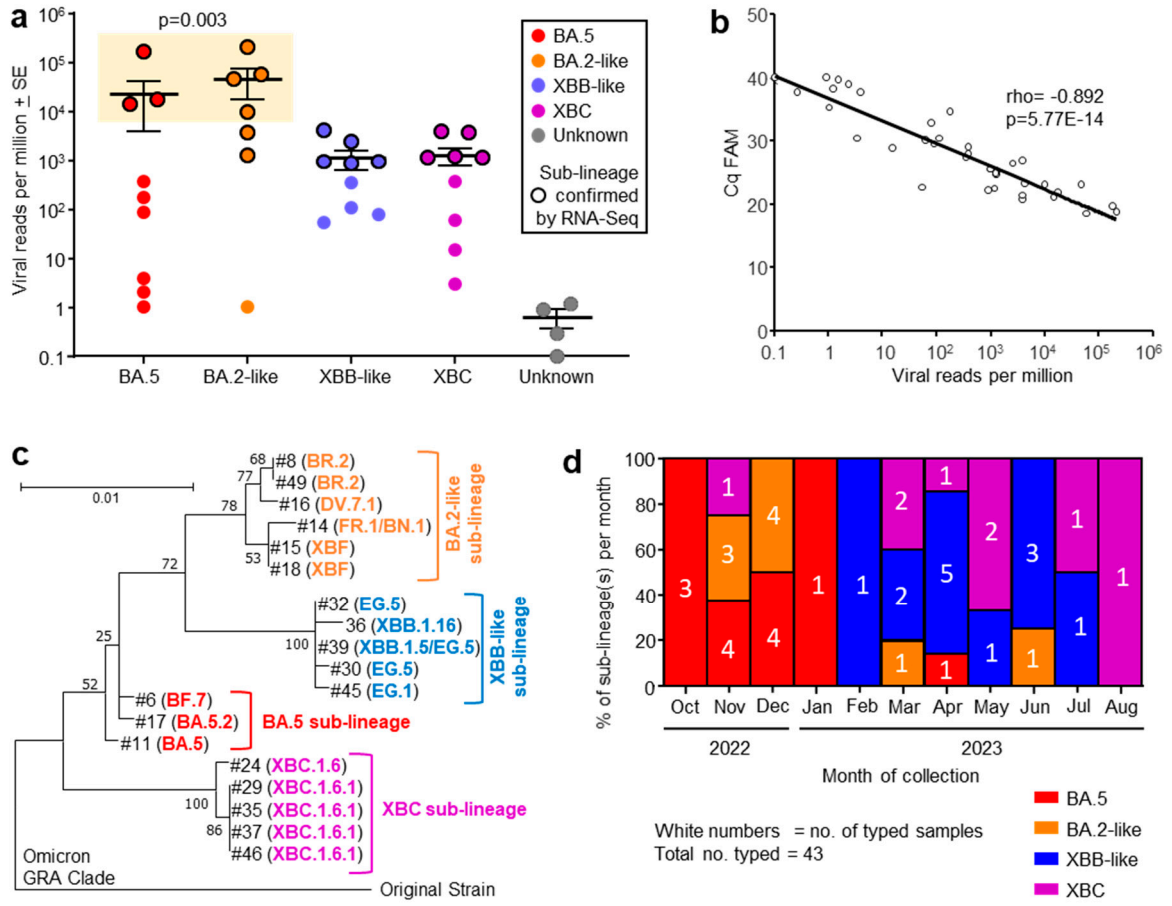

Figure 1. (**a**) Viral reads per million obtained from RNA-Seq for indicated omicron sublineages, with 4 samples having insufficient reads to allow classification (Unknown). Grouping was based on phylogeny (see c). The sublineage was determined by RT-PCR at the Royal Adelaide Hospital. Samples for which RNA-Seq confirmation of the sublineage was obtained are indicated by black outline. (**b**) Correlation between RT-qPCR (expressed as Cq FAM) and viral reads per million obtained from RNA-Seq, for the same nasopharyngeal swab samples. Spearman's correlation rho and p are provided. (**c**) Phylogenetic tree for SARS-CoV-2 spike protein sequences obtained from RNA-Seq data (n=19). Generated by MegaX. GISAID was used for sublineage classifications. (**d**) Percentage of each sublineage collected for each month for Oct 2022 to Aug 2023. The number of samples collected for each sublineage collected for each month are shown in white text.

3.4. Progression of Omicron Sublineages from Oct 2022 to Aug 2023

The number of patients infected with an identified sublineage was tracked month by month from Oct 2022 to Aug 2023, and is illustrated as a percentage of each sublineage per month (Fig. 1d). A clear progression was evident from BA.5 to BA.2-like to XBB-like and finally XBC (Fig. 1d), consistent with the global evolution of omicron sublineages [2–5,29].

3.5. Correlations of Viral Read Counts with Age and Other Patient Data

A range of patient data were collected and potential correlates sought. High viral RPM were significantly associated with patients who were ≥ 64 years of age (Fig. 2a), in agreement with previous reports [30,31]. Corticosteroid and baricitinib (JAK inhibitor) treatment showed no significant effect on viral RPM. Corticosteroid treatment is well established for reducing mortality [32], although a delay in viral clearance has been reported in some [33], but not other studies [34]. Baricitinib treatment also reduces mortality [35] and has been reported not to affect viral clearance [36]. All patients were treated with Remdesivir (SARS-CoV-2 antiviral).

 doi:10.20944/preprints202509.0565.v1

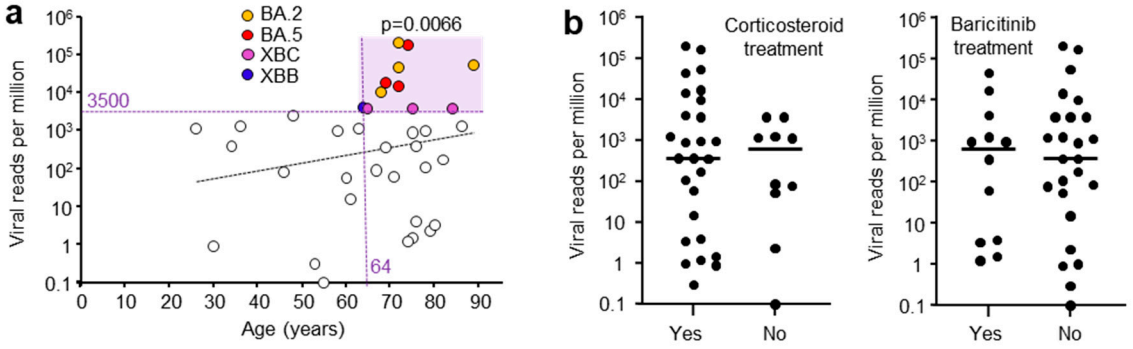

Figure 2. (**a**) Viral reads per million (RPM) and patient age. Viral RPM of >3500 RPM were significantly associated with patients that were ≥64 years of age (light purple shading). Statistics by Fischer's exact test (p=0.0066). (Dashed trend line did not reach significant). (**b**) Viral RPM for patients that received (Yes) or did not receive (No) corticosteroid or baricitnib (JAK inhibitor) treatment. Horizontal bars represent mean RPM. No significant differences were evident for Yes vs. No.

A series of other correlations failed to show significance. Whether the patients had received a COVID-19 vaccine did not significantly influence the mean viral RPM; however, only 3 patients did not receive a vaccine (Figure S1a). High viral RPM were associated with patients that had one or more comorbidities; however this did not reach significance, with only 5 patients free of comorbidities (Figure S1b). Previous studies have shown that patients with high viral loads often have comorbidities [37]. The length of stay in ICU or in hospital also did not correlate with viral RPM (Figure S1c), consistent with previous studies [38]. The viral RPM were not significantly different between males and females (Figure S1d). Viral loads are generally reported to be higher in females [39].

3.5. RNA-Seq Analysis of Human Gene Expression

There was sufficient RNA (≥100 ng) in 38/49 samples for RNA-Seq. RNA integrity number (RIN) scores ranged from 2.3 to 7.8 (mean 5.4 ± SD 1.4), illustrating that RNA in the nasopharynx, as might be expected, often suffers from a level of degradation. This is a recognized issue in many clinical samples, and can be ameliorated by depletion of ribosomal RNA, rather than enriching by poly(A) capture, prior to library generation [40,41]. Approximately 30 million reads were obtained for each sample with a mean of 75% aligning to the human reference genome (Table S1), illustrating that human gene expression data can be obtained from most nasopharyngeal swabs.

DeSeq2 was used to identify differentially expressed genes (DEGs) using pairwise comparisons between samples from patients infected with the different sublineages. This approach provided only a small number of DEGs for each comparison, with BA.5 vs. XBC providing the largest number of DEGs (n=43 DEGs with gene name annotations) (Table S2). No cogent pathways were identified by *inter alia* Ingenuity Pathway analysis (IPA) [23,42,43]. However, the top upregulated gene was Growth and differentiation factor 15 (GDF15) (Table S2) (a member of the TGF-β superfamily), which in COVID-19, increases with tissue damage [44]. As the mean viral RPM was ≈17 times higher in BA.5 compared with XBC (Fig. 1a), more tissue damage might be envisioned in the BA.5-infected cohort.

 doi:10.20944/preprints202509.0565.v1

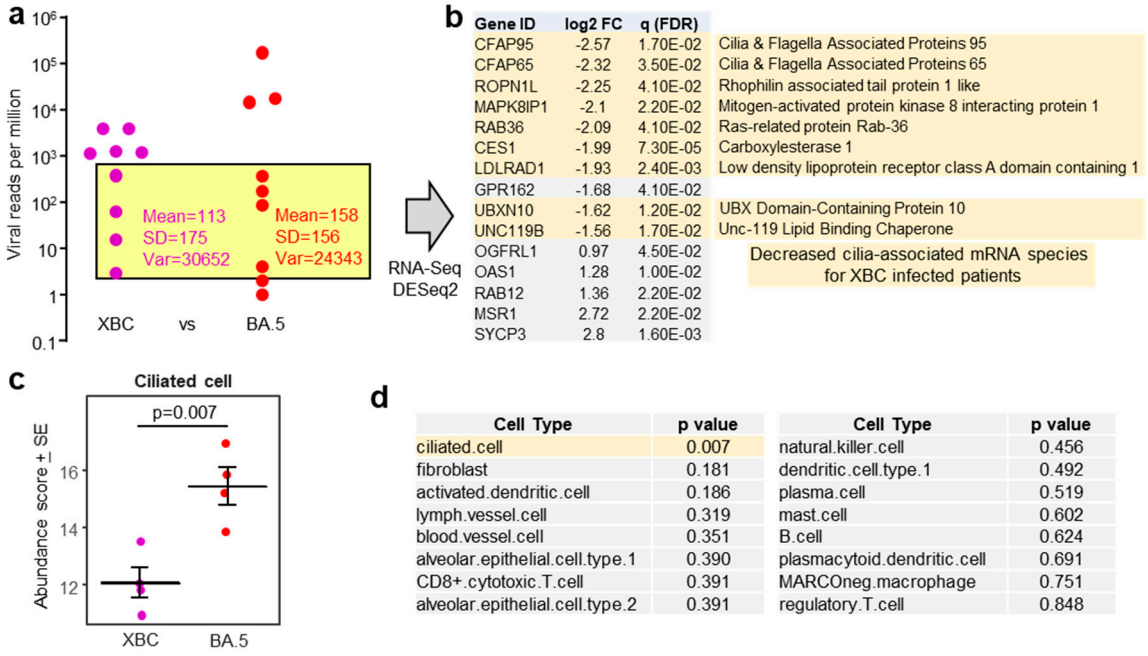

Figure 3. (**a**) Viral reads per million (RPM) are presented as in Fig. 1a, but with XBC placed to the left of BA.5. The samples in the yellow shaded box provided a XBC n=4 vs.BA.5 n=4 comparison for nasopharyngeal swabs with comparable viral loads, excluding samples with high and very low viral RPM. (**b**) For XBC vs. BA.5, most of the mRNA species (DEGs) significantly down-regulated in XBC samples (i.e. negative log2 Fold Change relative to XBC) were genes associated with cilia (pale yellow shading). (**c**) Relative abundance of ciliated cells as determined by cellular deconvolution using human lung cell atlas. Statistics by t test. (**d**) Full data set of cell types identified by cellular deconvolution, showing the cell types with significant (pale yellow shading) or non-significant (grey shading) differences in relative abundance between XBC and BA.5 samples. Statistics by t tests.

To mitigate against the influence of large differences in viral loads, patient samples with comparable viral RPM were compared for human gene expression (Fig. 3a, yellow shaded box). The exclusion of samples with high and very low viral RPM, left four XBC and four BA.5 samples (Fig. 3a). These 8 samples had slightly higher RIN scores (range 3.8 - 7.8, mean 5.6 ± SD 1.2). DeSeq2 again only identified a small number of DEGs; however 9/10 of the mRNA species that were down-regulated in XBC samples were associated with cilia (Fig. 3b). This analysis argues that more ciliated epithelial cells were infected and disrupted in the nasopharynx of XBC-infected patients than in BA.5-infected patients. The genes were the cilia-associated protein CFAP95 [45] and CFAP65 (expressed in lung [46]), ROPN1L [47], MAPK8IP1 [48], RAB36 (paralog of RAB34) [49], CES1 (highly expressed in ciliated epithelium [50]), LDLRAD1 [51], UBXN10 [52] and UNC119 [53].

Using the data from the same samples (Fig. 3a, yellow shading), but using the entire expression matrices (rather than just DEGs), cellular deconvolution analysis was undertaken to estimate the relative abundance of different cell types. Cell-type expression matrices for cells from the human nasopharynx (upper respiratory track) are not available, so cell-type expression matrices for human lung (lower respiratory track) were used. The abundance of ciliated cells emerged as significantly lower in XBC vs. BA.5 samples (Fig. 3c), consistent with the analysis of individual DEGs in Fig. 3b. Of all the cell types identified by cellular deconvolution, only the abundance of ciliated cells was significantly different between XBC and BA.5 samples (Fig. 3d).

4. Discussion

Herein we present viral and human gene expression data derived from nasopharyngeal swabs using RNA-Seq. Ribosomal depletion rather than poly(A) capture was used to ameliorate the problem of lower RNA quality (lower RIN scores, indicating some RNA degradation) [35,36]. The

 doi:10.20944/preprints202509.0565.v1

viral RPM correlated well with standard RT-qPCR viral load quantitation, providing a level of cross-validation of RT-qPCR and RNA-Seq data. High viral RPM were significantly associated with age ≥64, and patients with high viral RPM also often had comorbidities, data consistent with previous studies [30,31,37]. Immunosuppression with corticosteroids and/or baricitinib did not significantly influence viral RPM, results again consistent with previous studies [34,36]. Taken together, these data illustrate that viral RPM obtained via RNA-Seq provides reliable information on viral loads in the upper respiratory track. However, in this context RT-qPCR is currently clearly cheaper and more accessible and unlikely to be replaced by RNA-Seq.

The advantage of RNA-Seq is that it also provides gene expression data for the human host, with the data presented herein illustrating that a very respectable number of human mRNA reads can be obtained from nasopharyngeal swabs (Table S1). The very large range in viral loads may be due to a number of factors including sampling at different times during the course of the infections, differing effectiveness of anti-viral treatment or anti-viral immunity, and/or differing levels of the initial infectious viral inoculum. Although perhaps to be expected in any cohort of virus-infected patients, such large variability complicates the ability to generate salient comparisons of human gene expression between samples from patients infected with different sublineages. Large differences in the level of virus infection will have a much greater effect on gene expression than the more subtle differences that might emerge between infections with different subvariants of the same virus. Nevertheless, we illustrate that choosing patient samples with comparable viral RPM, allows generation of human differential gene expression data that reveals information about the biology of omicron sublineages. Specifically, that XBC infection in the nasopharynx resulted in significantly lower ciliated epithelial cell mRNA signatures when compared with BA.5 infection. Conceivably, the reduction in ciliated cell signatures might be associated, at least in part, with reprograming of gene expression in the infected cells [13]. However, XBC may simply infect and ultimately kill ciliated epithelial cells (via virus-induced cytopathic effects [54,55]) more efficiently than BA.5, leaving fewer of these cells available to be collected by the nasopharyngeal swabs.

5. Conclusions

RNA-Seq of human nasopharyngeal swabs provided evidence that the omicron sublineage XBC targets ciliated epithelial cells in the human upper respiratory track more effectively than BA.5. A key difference between the omicron lineage viruses and previous SARS-CoV-2 lineages was increased infection of ciliated epithelial cells in the upper respiratory track [13,14]. The data presented herein suggest that this evolutionary trend of increased targeting of ciliated cells continued as the omicron sublineage evolved from BA.5 to XBC.

Supplementary Materials: The following supporting information can be downloaded at the website of this paper posted on Preprints.org, Figure S1: Non-significant correlations with viral RPM; Table S1: RNA-Seq read data; Table S2. DEGs for pairwise comparisons between samples from different sublineages.

Author Contributions: Conceptualization, A.S., D.R.; methodology, A.S., C.R.B., M.P.P.; software, C.R.B.; formal analysis, C.R.B., A.S. A.C. ; investigation, A.C., M.P.P., E.R., S.C.B., C.M.H.; resources, B.G-B, M.P.P., A.S., D.J.R.; data curation, C.R.B., A.C.; writing—original draft preparation, A.C.; writing—review and editing, A.S.; visualization, A.C., A.S.; supervision, D.R., A.S., B.G-B, M.P.P., W.N.; project administration, A.S., D.R., B.G-B, M.P.P.; funding acquisition, A.S., D.R., B.G-B. All authors have read and agreed to the published version of the manuscript.

Funding: This research was funded by philanthropic donations for COVID-19 research from the Brazil Family Foundation, Australia, grant funding from The Hospital Research Foundation Group, Adelaide, Australia, and The Health Services Charitable Gifts Board, Adelaide, Australia. Prof A Suhrbier was awarded an Investigator grant by the National Health and Medical Research Council (NHMRC) of Australia (APP1173880). Agnes Carolin was a recipient of a PhD scholarship & fee waiver from the Faculty of Health, Medicine and Behavioral Sciences, University of Queensland, Brisbane, Australia.

 doi:10.20944/preprints202509.0565.v1

Institutional Review Board Statement: Approval was obtained from the Central Adelaide Local Health Network (CALHN) Human Research Ethics Committee and CALHN Research Governance (CALHN13050). Approval was also obtained from the QIMR Berghofer Human Research Ethics Committee (Ref: P3600). All sample and patient data was deidentified.

Informed Consent Statement: Informed consent was obtained from all subjects involved in the study.

Data Availability Statement: The RNA-Seq fastq files are available from NCBI SRA BioProject ID: PRJNA1313398.

Acknowledgments: The authors wish to thank Dr Gunter Hartel (QIMR Berghofer) for his help with statistics. The authors wish to thank Ms Kathleen Glasby, Ms Sarah Dohery, Ms Nerissa Brown, Ms Mahni Foster, Mr Connor Christie and Ms Paola Arce-Arango for biospecimen and data collection.

Conflicts of Interest: The authors declare no conflicts of interest. The funders had no role in the design of the study; in the collection, analyses, or interpretation of data; in the writing of the manuscript; or in the decision to publish the results.

Abbreviations

The following abbreviations are used in this manuscript:

COVID-19	Coronavirus Disease of 2019
SARS-CoV-2	Severe acute respiratory syndrome coronavirus 2
RT-qPCR	Reverse transcriptase quantitative polymerase chain reaction
RNA-Seq	Ribonucleic acid sequencing
mRNA	Messenger RNA
RIN	RNA integrity number
DEGs	Differentially expressed genes
RPM	Reads per million
FDR	False discovery rate (q)
FC	Fold change

References

1. Markov, P. V.; Ghafari, M.; Beer, M.; Lythgoe, K.; Simmonds, P.; Stilianakis, N. I.; Katzourakis, A., The evolution of SARS-CoV-2. *Nature Reviews Microbiology* **2023,** 21, 361-379. https://doi.org/10.1038/s41579-023-00878-2
2. Roemer, C.; Sheward, D. J.; Hisner, R.; Gueli, F.; Sakaguchi, H.; Frohberg, N.; Schoenmakers, J.; Sato, K.; O'Toole, Á.; Rambaut, A., et al., SARS-CoV-2 evolution in the Omicron era. *Nature Microbiology* **2023,** 8, 1952-1959. https://doi.org/10.1038/s41564-023-01504-w
3. Hu, B.; Chan, J. F.-W.; Liu, Y.; Liu, H.; Chen, Y.-X.; Shuai, H.; Hu, Y.-F.; Hartnoll, M.; Chen, L.; Xia, Y., et al., Divergent trajectory of replication and intrinsic pathogenicity of SARS-CoV-2 Omicron post-BA.2/5 subvariants in the upper and lower respiratory tract. *eBioMedicine* **2024,** 99, 104916. https://doi.org/10.1016/j.ebiom.2023.104916
4. Velavan, T. P.; Ntoumi, F.; Kremsner, P. G.; Lee, S. S.; Meyer, C. G., Emergence and geographic dominance of Omicron subvariants XBB/XBB.1.5 and BF.7 - the public health challenges. *Int J Infect Dis* **2023,** 128, 307-309. https://doi.org/10.1016/j.ijid.2023.01.024
5. Wang, Q.; Guo, Y.; Zhang, R. M.; Ho, J.; Mohri, H.; Valdez, R.; Manthei, D. M.; Gordon, A.; Liu, L.; Ho, D. D., Antibody neutralisation of emerging SARS-CoV-2 subvariants: EG.5.1 and XBC.1.6. *Lancet Infect Dis* **2023,** 23, e397-e398. https://doi.org/10.1016/s1473-3099(23)00555-8
6. Carabelli, A. M.; Peacock, T. P.; Thorne, L. G.; Harvey, W. T.; Hughes, J.; Peacock, S. J.; Barclay, W. S.; de Silva, T. I.; Towers, G. J.; Robertson, D. L., SARS-CoV-2 variant biology: immune escape, transmission and fitness. *Nat Rev Microbiol* **2023,** 21, 162-177. https://doi.org/10.1038/s41579-022-00841-7

 doi:10.20944/preprints202509.0565.v1

7. Dadonaite, B.; Brown, J.; McMahon, T. E.; Farrell, A. G.; Figgins, M. D.; Asarnow, D.; Stewart, C.; Lee, J.; Logue, J.; Bedford, T., et al., Spike deep mutational scanning helps predict success of SARS-CoV-2 clades. *Nature* **2024,** 631, 617-626. https://doi.org/10.1038/s41586-024-07636-1
8. Steiner, S.; Kratzel, A.; Barut, G. T.; Lang, R. M.; Aguiar Moreira, E.; Thomann, L.; Kelly, J. N.; Thiel, V., SARS-CoV-2 biology and host interactions. *Nature Reviews Microbiology* **2024,** 22, 206-225. https://doi.org/10.1038/s41579-023-01003-z
9. Gupta, S.; Gupta, D.; Bhatnagar, S., Analysis of SARS-CoV-2 genome evolutionary patterns. *Microbiology Spectrum* **2024,** 12, e02654-23. https://doi.org/10.1128/spectrum.02654-23
10. Ivanov, K. I.; Yang, H.; Sun, R.; Li, C.; Guo, D., The emerging role of SARS-CoV-2 nonstructural protein 1 (nsp1) in epigenetic regulation of host gene expression. *FEMS Microbiology Reviews* **2024,** 48, fuae023. https://doi.org/10.1093/femsre/fuae023
11. Garcia Lopez, V.; Plate, L., Comparative Interactome Profiling of Nonstructural Protein 3 Across SARS-CoV-2 Variants Emerged During the COVID-19 Pandemic. *Viruses* **2025,** 17, 447. https://doi.org/10.3390/v17030447
12. Takada, K.; Orba, Y.; Kida, Y.; Wu, J.; Ono, C.; Matsuura, Y.; Nakagawa, S.; Sawa, H.; Watanabe, T., Genes involved in the limited spread of SARS-CoV-2 in the lower respiratory airways of hamsters may be associated with adaptive evolution. *Journal of Virology* **2024,** 98, e01784-23. https://doi.org/10.1128/jvi.01784-23
13. Wu, C.-T.; Lidsky, P. V.; Xiao, Y.; Cheng, R.; Lee, I. T.; Nakayama, T.; Jiang, S.; He, W.; Demeter, J.; Knight, M. G., et al., SARS-CoV-2 replication in airway epithelia requires motile cilia and microvillar reprogramming. *Cell* **2023,** 186, 112-130.e20. https://doi.org/10.1016/j.cell.2022.11.030
14. Fonseca, B. F.; Robinot, R.; Michel, V.; Mendez, A.; Lebourgeois, S.; Chivé, C.; Jeger-Madiot, R.; Vaid, R.; Bondet, V.; Maloney, E., et al., Stealth replication of SARS-CoV-2 Omicron in the nasal epithelium at physiological temperature. *bioRxiv* **2025**, 2025.05.03.652024. https://doi.org/10.1101/2025.05.03.652024
15. Dumenil, T.; Le, T. T.; Rawle, D. J.; Yan, K.; Tang, B.; Nguyen, W.; Bishop, C.; Suhrbier, A., Warmer ambient air temperatures reduce nasal turbinate and brain infection, but increase lung inflammation in the K18-hACE2 mouse model of COVID-19. *Sci Total Environ* **2023,** 859, 160163. https://doi.org/10.1016/j.scitotenv.2022.160163
16. Dai, X.; Xu, R.; Li, N., The Interplay between Airway Cilia and Coronavirus Infection, Implications for Prevention and Control of Airway Viral Infections. *Cells* **2024,** 13, 1353. https://doi.org/10.3390/cells13161353
17. El-Daly, M. M., Advances and Challenges in SARS-CoV-2 Detection: A Review of Molecular and Serological Technologies. *Diagnostics* **2024,** 14, 519. https://doi.org/10.3390/diagnostics14050519
18. Pollak, N. M.; Rawle, D. J.; Yan, K.; Buckley, C.; Le, T. T.; Wang, C. Y. T.; Ertl, N. G.; van Huyssteen, K.; Crkvencic, N.; Hashmi, M., et al., Rapid inactivation and sample preparation for SARS-CoV-2 PCR-based diagnostics using TNA-Cifer Reagent E. *Frontiers in Microbiology* **2023,** 14, 1238542. https://doi.org/10.3389/fmicb.2023.1238542
19. Wu, Y.; Guo, Z.; Yuan, J.; Cao, G.; Wang, Y.; Gao, P.; Liu, J.; Liu, M., Duration of viable virus shedding and polymerase chain reaction positivity of the SARS-CoV-2 Omicron variant in the upper respiratory tract: a systematic review and meta-analysis. *International Journal of Infectious Diseases* **2023,** 129, 228-235. https://doi.org/https://doi.org/10.1016/j.ijid.2023.02.011
20. Stewart, R.; Yan, K.; Ellis, S. A.; Bishop, C. R.; Dumenil, T.; Tang, B.; Nguyen, W.; Larcher, T.; Parry, R.; Sng, J. J., et al., SARS-CoV-2 omicron BA.5 and XBB variants have increased neurotropic potential over BA.1 in K18-hACE2 mice and human brain organoids. *Front Microbiol* **2023,** 14, 1320856. https://doi.org/10.3389/fmicb.2023.1320856
21. Li, H.; Handsaker, B.; Wysoker, A.; Fennell, T.; Ruan, J.; Homer, N.; Marth, G.; Abecasis, G.; Durbin, R.; Genome Project Data Processing, S., The Sequence Alignment/Map format and SAMtools. *Bioinformatics* **2009,** 25, 2078-2079. https://doi.org/10.1093/bioinformatics/btp352
22. Love, M. I.; Huber, W.; Anders, S., Moderated estimation of fold change and dispersion for RNA-seq data with DESeq2. *Genome biology* **2014,** 15, 550. https://doi.org/10.1186/s13059-014-0550-8

23. Bishop, C. R.; Yan, K.; Nguyen, W.; Rawle, D. J.; Tang, B.; Larcher, T.; Suhrbier, A., Microplastics dysregulate innate immunity in the SARS-CoV-2 infected lung. *Frontiers in Immunology* **2024,** 15, 1382655. https://doi.org/10.3389/fimmu.2024.1382655
24. Danaher, P.; Kim, Y.; Nelson, B.; Griswold, M.; Yang, Z.; Piazza, E.; Beechem, J. M., Advances in mixed cell deconvolution enable quantification of cell types in spatial transcriptomic data. *Nature Communications* **2022,** 13, 385. https://doi.org/10.1038/s41467-022-28020-5
25. Madissoon, E.; Wilbrey-Clark, A.; Miragaia, R. J.; Saeb-Parsy, K.; Mahbubani, K. T.; Georgakopoulos, N.; Harding, P.; Polanski, K.; Huang, N.; Nowicki-Osuch, K., scRNA-seq assessment of the human lung, spleen, and esophagus tissue stability after cold preservation. *Genome biology* **2019,** 21, 1. https://doi.org/10.1186/s13059-019-1906-x
26. Vogels, C. B. F.; Brito, A. F.; Wyllie, A. L.; Fauver, J. R.; Ott, I. M.; Kalinich, C. C.; Petrone, M. E.; Casanovas-Massana, A.; Catherine Muenker, M.; Moore, A. J., et al., Analytical sensitivity and efficiency comparisons of SARS-CoV-2 RT–qPCR primer–probe sets. *Nature Microbiology* **2020,** 5, 1299-1305. https://doi.org/10.1038/s41564-020-0761-6
27. Robinson, J. T.; Thorvaldsdottir, H.; Turner, D.; Mesirov, J. P., igv.js: an embeddable JavaScript implementation of the Integrative Genomics Viewer (IGV). *Bioinformatics* **2023,** 39, btac830. https://doi.org/10.1093/bioinformatics/btac830
28. Scarpa, F.; Locci, C.; Azzena, I.; Casu, M.; Fiori, P. L.; Ciccozzi, A.; Giovanetti, M.; Quaranta, M.; Ceccarelli, G.; Pascarella, S., et al., SARS-CoV-2 recombinants: Genomic comparison between XBF and its parental lineages. *Microorganisms* **2023,** 11, 1824. https://doi.org/10.3390/microorganisms11071824
29. Chhoung, C.; Ko, K.; Ouoba, S.; Phyo, Z.; Akuffo, G. A.; Sugiyama, A.; Akita, T.; Sasaki, H.; Yamamoto, T.; Takahashi, K., et al., Sustained applicability of SARS-CoV-2 variants identification by Sanger Sequencing Strategy on emerging various SARS-CoV-2 Omicron variants in Hiroshima, Japan. *BMC Genomics* **2024,** 25, 1063. https://doi.org/10.1186/s12864-024-10973-0
30. To, K. K.-W.; Tsang, O. T.-Y.; Leung, W.-S.; Tam, A. R.; Wu, T.-C.; Lung, D. C.; Yip, C. C.-Y.; Cai, J.-P.; Chan, J. M.-C.; Chik, T. S.-H., et al., Temporal profiles of viral load in posterior oropharyngeal saliva samples and serum antibody responses during infection by SARS-CoV-2: an observational cohort study. *The Lancet Infectious Diseases* **2020,** 20, 565-574. https://doi.org/10.1016/S1473-3099(20)30196-1
31. Zhong, W.; Yang, X.; Jiang, X.; Duan, Z.; Wang, W.; Sun, Z.; Chen, W.; Zhang, W.; Xu, J.; Cheng, J., et al., Factors associated with prolonged viral shedding in older patients infected with Omicron BA.2.2. *Frontiers in Public Health* **2023,** 10, 1087800. https://doi.org/10.3389/fpubh.2022.1087800
32. Johns, M.; George, S.; Taburyanskaya, M.; Poon, Y. K., A Review of the Evidence for Corticosteroids in COVID-19. *Journal of Pharmacy Practice* **2021,** 35, 626-637. https://doi.org/10.1177/0897190021998502
33. Huang, R.; Zhu, C.; Jian, W.; Xue, L.; Li, C.; Yan, X.; Huang, S.; Zhang, B.; Zhu, L.; Xu, T., et al., Corticosteroid therapy is associated with the delay of SARS-CoV-2 clearance in COVID-19 patients. *European Journal of Pharmacology* **2020,** 889, 173556. https://doi.org/https://doi.org/10.1016/j.ejphar.2020.173556
34. Spagnuolo, V.; Guffanti, M.; Galli, L.; Poli, A.; Querini, P. R.; Ripa, M.; Clementi, M.; Scarpellini, P.; Lazzarin, A.; Tresoldi, M., et al., Viral clearance after early corticosteroid treatment in patients with moderate or severe covid-19. *Scientific Reports* **2020,** 10, 21291. https://doi.org/10.1038/s41598-020-78039-1
35. Patanwala, A. E.; Xiao, X.; Hills, T. E.; Higgins, A. M.; McArthur, C. J.; Alexander, G. C.; Mehta, H. B.; on behalf of National Covid Cohort Collaborative, C., Comparative Effectiveness of Baricitinib Versus Tocilizumab in Hospitalized Patients With COVID-19: A Retrospective Cohort Study of the National Covid Collaborative. *Critical Care Medicine* **2025,** 53, e29-41. https://doi.org/10.1097/CCM.0000000000006444
36. Viermyr, H.-K.; Tonby, K.; Ponzi, E.; Trouillet-Assant, S.; Poissy, J.; Arribas, J. R.; Dyon-Tafani, V.; Bouscambert-Duchamp, M.; Assoumou, L.; Halvorsen, B., et al., Safety of baricitinib in vaccinated patients with severe and critical COVID-19 sub study of the randomised Bari-SolidAct trial. *eBioMedicine* **2025,** 111, 105511. https://doi.org/10.1016/j.ebiom.2024.105511
37. Maltezou, H. C.; Raftopoulos, V.; Vorou, R.; Papadima, K.; Mellou, K.; Spanakis, N.; Kossyvakis, A.; Gioula, G.; Exindari, M.; Froukala, E., et al., Association Between Upper Respiratory Tract Viral Load,

 doi:10.20944/preprints202509.0565.v1

Comorbidities, Disease Severity, and Outcome of Patients With SARS-CoV-2 Infection. *The Journal of Infectious Diseases* **2021,** 223, 1132-1138. https://doi.org/10.1093/infdis/jiaa804

38. Cocconcelli, E.; Castelli, G.; Onelia, F.; Lavezzo, E.; Giraudo, C.; Bernardinello, N.; Fichera, G.; Leoni, D.; Trevenzoli, M.; Saetta, M., et al., Disease Severity and Prognosis of SARS-CoV-2 Infection in Hospitalized Patients Is Not Associated With Viral Load in Nasopharyngeal Swab. *Frontiers in Medicine* **2021,** 8, 714221. https://doi.org/10.3389/fmed.2021.714221
39. Liu, J.; Wen, R.; Wang, N.; Li, G.; Xu, P.; Li, X.; Zeng, X.; Liu, C., A retrospective study on COVID-19 infections caused by omicron variant with clinical, epidemiological, and viral load evaluations in breakthrough infections. *International Journal of Medical Sciences* **2024,** 21, 454. https://doi.org/10.7150/ijms.87167
40. Ura, H.; Niida, Y., Comparison of RNA-Sequencing Methods for Degraded RNA. *Int J Mol Sci* **2024,** 25, 6143. https://doi.org/10.3390/ijms25116143
41. Lu, W.; Zhou, Q.; Chen, Y., Impact of RNA degradation on next-generation sequencing transcriptome data. *Genomics* **2022,** 114, 110429. https://doi.org/https://doi.org/10.1016/j.ygeno.2022.110429
42. Carolin, A.; Frazer, D.; Yan, K.; Bishop, C. R.; Tang, B.; Nguyen, W.; Helman, S. L.; Horvat, J.; Larcher, T.; Rawle, D. J., et al., The effects of iron deficient and high iron diets on SARS-CoV-2 lung infection and disease. *Frontiers in Microbiology* **2024,** 15, 1441495. https://doi.org/10.3389/fmicb.2024.1441495
43. Carolin, A.; Yan, K.; Bishop, C. R.; Tang, B.; Nguyen, W.; Rawle, D. J.; Suhrbier, A., Tracking inflammation resolution signatures in lungs after SARS-CoV-2 omicron BA.1 infection of K18-hACE2 mice. *PLOS ONE* **2024,** 19, e0302344. https://doi.org/10.1371/journal.pone.0302344
44. Rochette, L.; Zeller, M.; Cottin, Y.; Vergely, C., GDF15: an emerging modulator of immunity and a strategy in COVID-19 in association with iron metabolism. *Trends Endocrinol Metab* **2021,** 32, 875-889. https://doi.org/10.1016/j.tem.2021.08.011
45. Andersen, J. S.; Vijayakumaran, A.; Godbehere, C.; Lorentzen, E.; Mennella, V.; Schou, K. B., Uncovering structural themes across cilia microtubule inner proteins with implications for human cilia function. *Nature Communications* **2024,** 15, 2687. https://doi.org/10.1038/s41467-024-46737-3
46. Wang, W.; Tu, C.; Nie, H.; Meng, L.; Li, Y.; Yuan, S.; Zhang, Q.; Du, J.; Wang, J.; Gong, F., et al., Biallelic mutations in CFAP65 lead to severe asthenoteratospermia due to acrosome hypoplasia and flagellum malformations. *J Med Genet* **2019,** 56, 750-757. https://doi.org/10.1136/jmedgenet-2019-106031
47. Liu, Y.; Liu, T.; Ruan, L.; Zhu, D.; He, Y.; Jia, J.; Chen, Y., Cilia Plays a Pivotal Role in the Hypersecretion of Airway Mucus in Mice. *Current Molecular Pharmacology* **2024,** 17, E18761429368288. https://doi.org/10.2174/0118761429368288250401054301
48. Verhey, K. J.; Hammond, J. W., Traffic control: regulation of kinesin motors. *Nature Reviews Molecular Cell Biology* **2009,** 10, 765-777. https://doi.org/10.1038/nrm2782
49. Ganga, A. K.; Kennedy, M. C.; Oguchi, M. E.; Gray, S.; Oliver, K. E.; Knight, T. A.; De La Cruz, E. M.; Homma, Y.; Fukuda, M.; Breslow, D. K., Rab34 GTPase mediates ciliary membrane formation in the intracellular ciliogenesis pathway. *Curr Biol* **2021,** 31, 2895-2905.e7. https://doi.org/10.1016/j.cub.2021.04.075
50. Li, R.; Liclican, A.; Xu, Y.; Pitts, J.; Niu, C.; Zhang, J.; Kim, C.; Zhao, X.; Soohoo, D.; Babusis, D., et al., Key Metabolic Enzymes Involved in Remdesivir Activation in Human Lung Cells. *Antimicrobial Agents and Chemotherapy* **2021,** 65, 10.1128/aac.00602-21. https://doi.org/10.1128/aac.00602-21
51. Geremek, M.; Bruinenberg, M.; Ziętkiewicz, E.; Pogorzelski, A.; Witt, M.; Wijmenga, C., Gene expression studies in cells from primary ciliary dyskinesia patients identify 208 potential ciliary genes. *Human Genetics* **2011,** 129, 283-293. https://doi.org/10.1007/s00439-010-0922-4
52. Raman, M.; Sergeev, M.; Garnaas, M.; Lydeard, J. R.; Huttlin, E. L.; Goessling, W.; Shah, J. V.; Harper, J. W., Systematic proteomics of the VCP–UBXD adaptor network identifies a role for UBXN10 in regulating ciliogenesis. *Nature Cell Biology* **2015,** 17, 1356-1369. https://doi.org/10.1038/ncb3238
53. Jean, F.; Pilgrim, D., Coordinating the uncoordinated: UNC119 trafficking in cilia. *European Journal of Cell Biology* **2017,** 96, 643-652. https://doi.org/https://doi.org/10.1016/j.ejcb.2017.09.001

 doi:10.20944/preprints202509.0565.v1

54. Tanneti, N. S.; Patel, A. K.; Tan, L. H.; Marques, A. D.; Perera, R. A. P. M.; Sherrill-Mix, S.; Kelly, B. J.; Renner, D. M.; Collman, R. G.; Rodino, K., et al., Comparison of SARS-CoV-2 variants of concern in primary human nasal cultures demonstrates Delta as most cytopathic and Omicron as fastest replicating. *mBio* **2024,** 15, e03129-23. https://doi.org/doi:10.1128/mbio.03129-23
55. Zaderer, V.; Abd El Halim, H.; Wyremblewsky, A.-L.; Lupoli, G.; Dächert, C.; Muenchhoff, M.; Graf, A.; Blum, H.; Lass-Flörl, C.; Keppler, O. T., et al., Omicron subvariants illustrate reduced respiratory tissue penetration, cell damage and inflammatory responses in human airway epithelia. *Frontiers in Immunology* **2023,** 14, 1258268. https://doi.org/10.3389/fimmu.2023.1258268